(21) G. M. Bancroft, I. Adams, L. L. Coatsworth, C. D. Bennewitz, J. D. Brown, and W. P. Westwood, *Anal. Chem.*, **47**, 586 (1975).
(22) A. Vogler in "Concepts of Inorganic Photochemistry", A. W. Adamson and P. D. Fleischauer, Ed., Wiley-Interscience, New York, N.Y., 1975, Chapter 6.
(23) R. Manne and T. Aberg, *Chem. Phys. Lett.*, **7**, 282 (1970).
(24) K. S. Kim, *J. Electron Spectrosc. Relat. Phenom.*, **3**, 217 (1974).
(25) H. Basch in "Metal-Ligand Interactions in Organic Chemistry and Biochemistry", B. Pullman and N. Goldblum, Ed., D. Reidel Publishing Co., Dordrecht, Holland, 1976.
(26) U. Gelius, *J. Electron Spectrosc. Relat. Phenom.*, **5**, 985 (1974).
(27) This is not true for Mo 3d, but there is a large error on the very weak Mo $3d_{5/2}$ shake-up peak (Figure 1b).
(28) S. Larsson and M. L. de Siqueirra, *Chem. Phys. Lett.*, **44**, 537 (1976).

Contribution from the Department of Inorganic Chemistry, University of Melbourne, Parkville 3052, Victoria, Australia

Kinetic and Thermodynamic Study of Reactions of Some Substituted Manganese(I) and Manganese(II) Tricarbonyl Complexes Using Spectrophotometric and Electrochemical Techniques

A. M. BOND,* B. S. GRABARIC,[1] and ZORANA GRABARIC[1]

Received September 8, 1977

Electrochemical oxidation and reduction processes enable the species *fac*-$[Mn(CO)_3(L\text{-}L')X]^{0,+}$ and *mer*-$[Mn(CO)_3(L\text{-}L']^{0,+}$ to be synthesized and their thermodynamic and kinetic properties to be studied via electrochemical and spectrophotometric measurements ((L-L') = bidentate phosphorus or arsenic ligand: X = Cl or Br). In oxidation state II, the 17-electron manganese complexes are extremely labile and several reactions occur. The rate of isomerism, *fac*-Mn(II) → *mer*-Mn(II), studied by a fully computerized version of double potential step chronoamperometry, is not markedly dependent on solvent, bidentate ligand, or X. A twist mechanism is proposed to explain this isomerism. By contrast the activation energy in the thermodynamically favored 18-electron oxidation state I isomerism must be extremely high because no isomerism was observed to occur in 24 h. *mer*-Mn(II) complexes generated via *fac*-Mn(II) isomerism undergo slow solvolysis and redox reactions in the dark. They are also extremely light sensitive and are rapidly reduced in sunlight. Reactions of manganese(II) carbonyls are therefore considerably more complex than previously thought.

In 1963 Angelici et al.[2] examined the isomerism of a series of $Mn(CO)_3(L)_2X$ (L = ligand, X = Cl, Br, I) complexes. In these 18-electron manganese(I) systems, it was concluded that isomerism occurred via an intermolecular mechanism involving the dissociation of L.

With the complexes $Mn(CO)_3$dpmX (dpm = bis(diphenylphosphino)methane; X = Cl, Br) the usually synthesized form is the facial isomer.[3] Recently, Bond et al.[4] demonstrated that on electrochemical oxidation a 17-electron facial manganese(II) complex *fac*-$[Mn(CO)_3dpmX]^+$ can be generated which subsequently isomerizes to *mer*-$[Mn(CO)_3dpmX]^+$. The *mer*-Mn(II) species was then in turn shown to react with the solvent to form *mer*-$Mn(CO)_3$dpmX which subsequently decomposed via loss of carbon monoxide rather than isomerizing to the usually isolated *fac*-$Mn(CO)_3$dpmX complex. Thus, using electrochemical techniques, each of the isomers in the 18- and 17-electron configuration can be prepared and their chemical reactions studied. The opportunity therefore exists to examine from both a thermodynamic and kinetic viewpoint the differences between the 17- and 18-electron manganese systems and to consider whether the reactions in the different oxidation states occur via the same mechanisms and pathways.

From the preceding work, the above study appeared to require a quantitative description of the reaction scheme

$$\begin{array}{ccc} \textit{fac}\text{-Mn(I)} & \overset{k_{s1},\,E_1^\circ}{\rightleftharpoons} & \textit{fac}\text{-Mn(II)} \\ k_2,\ \Delta G_2^\circ \uparrow\downarrow k_2'' & & k_1' \uparrow\downarrow k_1,\ \Delta G_1^\circ \\ \text{loss of CO} \overset{k_4}{\leftarrow} \textit{mer}\text{-Mn(I)} & \overset{k_{s2},\,E_2^\circ}{\rightleftharpoons} & \textit{mer}\text{-Mn(II)} + \text{solvent} \overset{k_3}{\rightarrow} \textit{mer}\text{-Mn(I)} \end{array}$$

in various solvents and under various conditions, where k_{sn} = heterogeneous electron transfer rate constant, k_n = homogeneous chemical rate constant for designated chemical step, and other symbols have their usual meaning. However, during the course of this work it was discovered that the *mer*-Mn(II) complexes are extremely light sensitive and that reduction to Mn(I) and solvolysis can be catalyzed quite markedly by the presence of light. Additional measurements to include the light-sensitive pathways were therefore needed.

To examine the influence of the substitutents on the thermodynamic and kinetic aspects of the various processes the following bidentate ligands were chosen for the tricarbonyl systems: bis(diphenylphosphino)methane (dpm), 1,2-bis(diphenylphosphino)ethane (dpe), 1,2-bis(diphenylarsino)ethane (dae), 1-diphenylphosphino-2-diphenylarsinoethane (ape). Each of these ligands was used with both chloride and bromide and various studies were made in acetone, acetonitrile, dichloromethane, and propylene carbonate. Since each of the isomers is highly colored, conventional spectrophotometric monitoring of the various species as a function of time is possible. However, the *fac*-Mn(II) → *mer*-Mn(II) isomerism step was too fast at room temperature to be studied conveniently by spectrophotometry and the electrochemical technique of double potential step chronoamperometry[5] was used. With this technique, correction for charging current and the calculations themselves are usually difficult or extremely tedious to perform. However, a completely computerized on-line system has been developed to perform all the required tasks, and accurate rate constants have been obtained via a highly convenient method. For other reactions a novel combination of spectrophotometric monitoring of species and highly specific electrochemical quenching of another reaction pathway enables the distinction to be made between steps that normally occur with similar rates.

Experimental Section

Preparation of Compounds and Solutions. The preparation of the yellow *fac*-$Mn(CO)_3(L\text{-}L')X$ was undertaken essentially by the method of Colton and McCormick.[6] Initially $Mn(CO)_5Cl$ or $Mn(CO)_5Br$ was prepared by passing chlorine through a dichloromethane solution of $Mn_2(CO)_{10}$ or adding bromine dropwise to the $Mn_2(CO)_{10}$ solution, respectively. The purity of the products was monitored by infrared spectroscopy. $Mn(CO)_5X$ was then refluxed with a stoichiometric amount of dpm, dpe, dae, or ape (Strem Chemicals) in *n*-hexane to give *fac*-$Mn(CO)_3(L\text{-}L')X$ complexes which were recrystallized from dichloromethane. Infrared data on the purified complexes in dichloromethane were consistent with those for the facial isomer.[4]

0020-1669/78/1317-1013$01.00/0

Solutions of the *mer*-$[Mn(CO)_3(L\text{-}L')X]^+$ complexes (red for X = Cl, purple for X = Br) were quantitatively prepared in the solvent/electrolyte being studied by controlled potential electrolysis of *fac*-$Mn(CO)_3(L\text{-}L')X$ at 25 °C under argon using a PAR potentiostat/galvanostat Model 173. Platinum gauze was used as the working electrode and auxiliary electrode while Ag|AgCl (0.1 M LiCl; acetone) was the reference electrode. The auxiliary electrode was filled with a solution of the supporting electrolyte/solvent and was separated from the solution to be electrolyzed by a porous vycor sinter. A salt bridge, also containing the supporting electrolyte/solvent, was used to separate the reference electrode from the solution to be electrolyzed. A potential of +1.6 V vs. Ag|AgCl was applied to the working electrode and because the complexes were found to be light sensitive the cell was covered with aluminum foil at all stages of the electrolysis. The starting materials were yellow and with X = Cl red solutions of the cation were obtained whereas with X = Br the cations are purple. Cyclic voltammograms of the product were used to verify that *mer*-$[Mn(CO)_3(L\text{-}L')X]^+$ had been obtained and that all of the starting material had been oxidized. Solutions were generated as required and used immediately after preparation. Chemical isolation of the cations as PF_6^- salts can be achieved by $NOPF_6$ oxidation as reported for the dpm case,[4] but electrochemical generation of materials, as required, was considered to be more convenient. With ape, two *mer* configurations are possible, but no assignment could be made from infrared measurements.

Yellow *mer*-$Mn(CO)_3(L\text{-}L')X$ solutions were prepared quantitatively by controlled potential reduction of *mer*-$[Mn(CO)_3(L\text{-}L')X]^+$ at +0.6 V vs. Ag|AgCl. As for the *fac*-$Mn(CO)_3(L\text{-}L')X$ species, these complexes are yellow in color. The course of this reaction was again monitored by cyclic voltammetry.

While *fac*-$[Mn(CO)_3(L\text{-}L')X]^+$ can be identified as an intermediate in the preparation of the *mer*-$[Mn(CO)_3(L\text{-}L')X]^+$ complex, because of the rapid isomerism, stable solutions of this species could not be prepared. Reactions of this species were therefore studied by examination of changes in surface concentrations at the electrode surface as a function of time.

All solvents used were of analytical reagent grade purity and tetraethylammonium perchlorate, Et_4NClO_4, was used as the supporting electrolyte in all work. The concentration of Et_4NClO_4 was 0.1 M in all solvents except for dichloromethane where a concentration of 0.07 M was employed.

Instrumentation. (i) Spectrophotometric. Spectrophotometric measurements were made with a Varian Techtron Model 635D UV–vis spectrophotometer using either 1-cm or 1-mm matched cells. The reference cell contained the same solvent/electrolyte as the test solution.

(ii) Electrochemical. Voltammograms were recorded with either a PAR (Princeton Applied Research Corporation, N.J.) 170 electrochemistry system or Model 174 polarographic analyzer. Platinum wire was used for both the working electrode and auxiliary electrode and Ag|AgCl (0.1 M LiCl:acetone) was used as the reference electrode. The reference electrode was separated from the test solution by a salt bridge containing the same solvent/supporting electrolyte as used in the test solution. All measurements were performed using positive feedback circuitry to minimize the *iR* drop. Platinum working electrodes were cleaned in 1 M nitric acid, rinsed with water, and then rinsed with solvent prior to performing initial experiments. Between replicate experiments, wiping of electrodes with a tissue was undertaken.

The computerized instrumentation for double potential step chronoamperometry utilized a PDP 11/10 (Digital Equipment Corp.) minicomputer (CAPS-11 System) interfaced to a PAR Model 174 polarographic analyzer. Nonstandard features used with the CAPS-11 system were the following: (1) AR 11, one-module real-time analogue subsystem which includes a 16-channel 10-bit A/D converter with sample-and-hold circuitry, a programmable real-time clock, and display control with two 10-bit D/A converters; (2) DR 11, a general purpose interface for program-controlled 16-bit parallel I/O transfers; (3) an interface made with two serial 8-bit (i.e., 16-bit wide) D/A converters for generating program-controlled pulses from DR 11. The pulses were fed through an external imput into the PAR 174 polarographic analyzer. The main computer program was written in BASIC language. Potential steps, current sampling times, t, and pulse duration, τ, were program controlled. The current was sampled approximately each 3 ms and the pulse duration was 100 ms or greater.

The first pulse oxidized the *fac*-Mn(I) complex and the second one reduced whatever *fac*-Mn(II) remained after the application of the initial potential step. After the current–time curves for oxidation and reduction were stored in memory, the same experiment was performed with the solvent/electrolyte solution and the charging current correction was obtained by subtraction of the second set of data. The current–time behavior for the oxidation of *fac*-Mn(I) complex was diffusion controlled (plot of current vs. $t^{-1/2}$ was linear and passing through the origin within a few percent) for all systems. Theoretical calculation of the ratio of cathodic to anodic currents vs. $k\tau$ (k being first-order rate constant) was then undertaken using the theory of Schwarz and Shain[5] for different values of $(t - \tau)/\tau$ assuming planar diffusion. Experimentally obtained ratios of cathodic to anodic currents for each value of $(t - \tau)/\tau$ was interpolated from the theoretical curve and a set of 20 values of rate constants was evaluated for every system. Reported values of k are mean values obtained from three sets of 20 values with corresponding standard deviations.

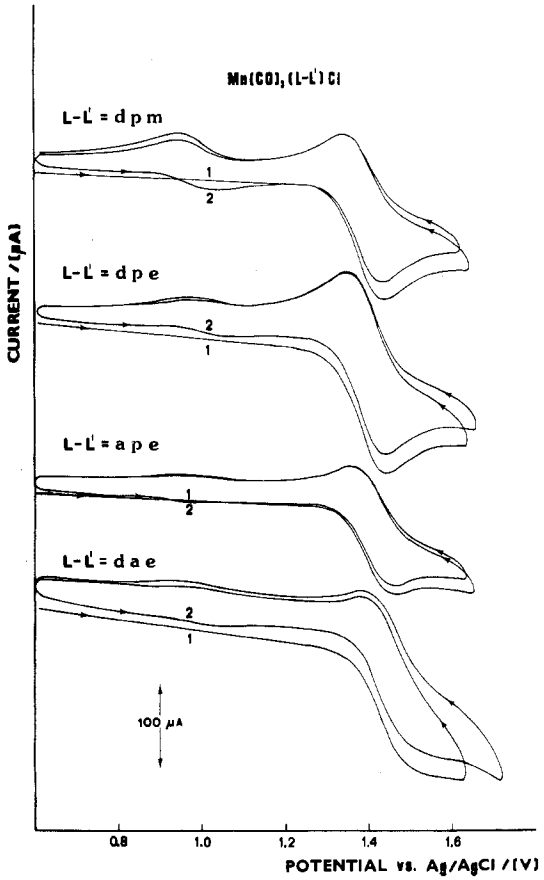

Figure 1. Cyclic voltammograms at a platinum electrode for a number of *fac*-$Mn(CO)_3(L\text{-}L')X$ complexes at 25 °C in acetonitrile (0.1 M Et_4NClO_4). Scan rate = 500 mV/s.

All current–time data were displayed on a Tektronix D13 storage-oscilloscope and/or X-Y recorder.

Further details of the instrumentation and procedures used in this on-line experiment for calculating chemical rate constants for reactions following electron transfer can be obtained by writing to the authors.

Results and Discussion

Thermodynamics and Kinetics of the Electron-Transfer Steps. Figure 1 shows cyclic voltammograms for oxidation of a number of *fac*-$Mn(CO)_3(L\text{-}L')X$ complexes at 25 °C in acetonitrile. Oxidation occurs at about 1.4 V vs. Ag|AgCl and the electrode process is[4]

$$fac\text{-Mn(I)} \overset{-e}{\rightleftarrows} fac\text{-Mn(II)} \rightarrow mer\text{-Mn(II)}$$

The new wave present at less positive potentials on second and subsequent scans is the

$$mer\text{-Mn(II)} \overset{+e}{\rightleftarrows} mer\text{-Mn(I)}$$

step.[4]

Table I. E_2° and E_1° Values[a]

Compound	Solvent			
	CH_3CN	C_3H_6O	CH_2Cl_2	$C_4H_6O_3$
(a) E_2° [*mer*-Mn(I)/*mer*-Mn(II)], V vs. Ag|AgCl (Meridional Isomer)				
$Mn(CO)_3$dpmCl	+0.95	+0.94		
$Mn(CO)_3$dpmBr	+0.97	+0.97	+1.03	+0.95
$Mn(CO)_3$dpeCl	+1.02	+1.00		
$Mn(CO)_3$dpeBr	+1.02	+1.03		
$Mn(CO)_3$apeCl	+1.00	+1.02		
$Mn(CO)_3$apeBr	+1.06	+1.03		
$Mn(CO)_3$daeCl	+1.00	+1.00		
$Mn(CO)_3$daeBr	+1.00	+1.02		
(b) E_1° [*fac*-Mn(I)/*fac*-Mn(II)], V vs. Ag|AgCl (Facial Isomer)				
$Mn(CO)_3$dpmCl	+1.48	+1.41		
$Mn(CO)_3$dpmBr	+1.41	+1.45	+1.45	+1.37
$Mn(CO)_3$dpeCl	+1.37	+1.41		
$Mn(CO)_3$dpeBr	+1.41	+1.48		
$Mn(CO)_3$apeCl	+1.43	+1.44		
$Mn(CO)_3$apeBr	+1.45	+1.46		
$Mn(CO)_3$daeCl	+1.45	+1.47		
$Mn(CO)_3$daeBr	+1.47	+1.49		

[a] $T = 25$ °C; supporting electrolyte Et_4NClO_4; scan rate = 500 mV/s. Oxidation of Mn(II) and reduction of Mn(I) was also observed as described for the $Mn(CO)_3$dpm X complex in ref 4.

Figure 2 shows the reduction of *mer*-$[Mn(CO)_3$dpeBr$]^+$ and oxidation of *mer*-$Mn(CO)_3$dpeBr in acetonitrile. The *mer*-Mn(I)/*mer*-Mn(II) couple is both electrochemically and chemically reversible for all ligands, L-L′, and X at 25 °C under conditions of cyclic voltammetry with a scan rate up to 1 V/s.

Assuming equal diffusion coefficients for reduced and oxidized forms, the E_2° value for the

$$mer\text{-}[Mn(CO)_3(L\text{-}L')X]^+ + e \underset{}{\overset{k_{s_2},\,E_2^\circ}{\rightleftharpoons}} mer\text{-}Mn(CO)_3(L\text{-}L')X$$

couple is therefore easily calculated from the potential at 85.2% of the peak height for reduction or oxidation steps in cyclic voltammograms. Values of E_2° in various solvents are contained in Table Ia. From the cyclic voltammetric data the heterogeneous rate constant for electron transfer k_{s_2} must be $\geq 10^{-1}$ cm s^{-1} for all complexes in all solvents.

The oxidation step at +1.4 V vs. Ag|AgCl as shown in Figure 1 is clearly neither chemically or electrochemically reversible under conditions of cyclic voltammetry and therefore E_1° cannot be measured directly from these current–potential curves. The electrode process can be written as

$$fac\text{-}Mn(CO)_3(L\text{-}L')X \overset{E_1^\circ,\,k_{s_1}}{\rightleftharpoons} fac\text{-}[Mn(CO)_3(L\text{-}L')X]^+ \overset{k_1}{\longrightarrow} mer\text{-}[Mn(CO)_3(L\text{-}L')X]^+$$

assuming no other side reactions are important on the electrochemical time scale (see later data and discussion for proof of this). Both k_{s_1} and k_1 are dependent on the complex and solvent and to compute E_1° their influence must be taken into account. Using values of k_1 calculated via double potential step chronoamperometry (see later) and digital simulation of the cyclic voltammetric response using procedures described by Feldberg[7] with various k_{s_2} and known k_1 values enabled the value of E_1° to be calculated. Values are given in Table Ib. k_{s_1} values in the range 5×10^{-2} to 10^{-2} cm s^{-1} were found for the couple

$$fac\text{-}Mn(CO)_3(L\text{-}L')X \overset{E_1^\circ,\,k_{s_1}}{\rightleftharpoons} fac\text{-}[Mn(CO)_3(L\text{-}L')X]^+$$

Some interesting features arise from the thermodynamic and kinetic calculations of the electron-transfer step. It is apparent that the E_1° and E_2° values are within the limit of experimental error essentially independent of ligand or solvent. This suggests that the energy differences between the oxidized and reduced forms are not markedly altered by varying the ligand. The values of $(E_2^\circ - E_1^\circ)$ enable the equilibrium constant for the reaction

$$fac\text{-}Mn(II) + mer\text{-}Mn(I) \overset{K}{\rightleftarrows} fac\text{-}Mn(I) + mer\text{-}Mn(II)$$

to be calculated. Results are summarized in Table II for $Mn(CO)_3$dpmBr and it can be seen that the equilibrium position is a long way to the right in all solvents. The large difference in E_1° and E_2° is therefore attributable to the very high thermodynamic stability of *fac*-Mn(I) and *mer*-Mn(II) relative to their counterparts in the alternative oxidation state.

The fact that k_{s_1} is considerably less than k_{s_2} is difficult to rationalize. Double layer corrections seem unlikely to account for the difference. The possibility that the 17-electron *fac*-Mn(II) species is a relatively more fluxional molecule than some of the other species may be consistent with the observation. Certainly the *fac*-Mn(II) species is kinetically labile in terms of its rate of isomerism and it may be that the *fac*-Mn(I)/*fac*-Mn(II) couple involves some structural rearrangements which are not so important in the *mer*-Mn(I)/*mer*-Mn(II) couple. Adequate structural information on the four species is not available to test this hypothesis.

Table II. Equilibrium Constants for the $Mn(CO)_3$dpmBr System

$$fac\text{-}Mn(II) + mer\text{-}Mn(I) \overset{K}{\rightleftarrows} fac\text{-}Mn(I) + mer\text{-}Mn(II)$$

in Different Solvents ($T = 25$ °C)

Solvent	log K
CH_3CN(0.1 M Et_4NClO_4)	7.4
CH_2Cl_2(0.07 M Et_4NClO_4)	7.1
C_3H_6O(0.1 M Et_4NClO_4)	8.1
$C_4H_6O_3$(0.1 M Et_4NClO_4)	7.1

Table III. Values of k_1 for Isomerism of *fac*-$[Mn(CO)_3(L\text{-}L')X]^+$ Obtained in Acetonitrile (0.1 M Et_4NClO_4) at Various Temperatures (Concentration of *fac*-$Mn(CO)_3(L\text{-}L')X = 10^{-3}$ M)

Compd (*fac* isomer)	k_1, s^{-1}		
	25 °C	35 °C	45 °C
$[Mn(CO)_3$dpmCl$]^+$	2.4 ± 0.2	5.5 ± 0.5	10 ± 1
$[Mn(CO)_3$dpmBr$]^+$	7.5 ± 0.9	12 ± 2	22 ± 2
$[Mn(CO)_3$dpeCl$]^+$	2.5 ± 0.2	3.4 ± 0.4	10 ± 1
$[Mn(CO)_3$dpeBr$]^+$	1.5 ± 0.1	2.2 ± 0.1	4.8 ± 0.5
$[Mn(CO)_3$apeCl$]^+$	1.9 ± 0.3	5.3 ± 0.6	13 ± 2
$[Mn(CO)_3$apeBr$]^+$	2.0 ± 0.2	3.2 ± 0.4	8.0 ± 1.0
$[Mn(CO)_3$daeCl$]^+$	4.2 ± 0.5	15 ± 3	*a*
$[Mn(CO)_3$daeBr$]^+$	2.0 ± 0.3	7.0 ± 1.0	16 ± 2

[a] Too fast to measure.

Table IV. k_1 Values Obtained for Isomerism of *fac*-$[Mn(CO)_3$dpmCl$]^+$ in Various Solvents with Et_4NClO_4 as Supporting Electrolyte at 25 °C

Solvent	k_1, s^{-1}	Solvent	k_1, s^{-1}
CH_3CN	2.4 ± 0.2	CH_2Cl_2	4.2 ± 0.3
C_3H_6O	5.5 ± 0.5	$C_4H_6O_3$	3.1 ± 0.3

Kinetics and Thermodynamics of Isomerism. (i) *fac*-Mn(II) → *mer*-Mn(II). Figure 3 shows the temperature dependence of the cyclic voltammograms of $Mn(CO)_3$dpeBr in acetonitrile. The electrode process is

$$fac\text{-}Mn(CO)_3(L\text{-}L')X \rightleftarrows fac\text{-}[Mn(CO)_3(L\text{-}L')X]^+$$

$$fac\text{-}[Mn(CO)_3(L\text{-}L')X]^+ \overset{k_1}{\longrightarrow} mer\text{-}[Mn(CO)_3(L\text{-}L')X]^+$$

and clearly the rate of isomerism increases significantly with increase in temperature. Data obtained in acetonitrile at various temperatures via the computerized double potential

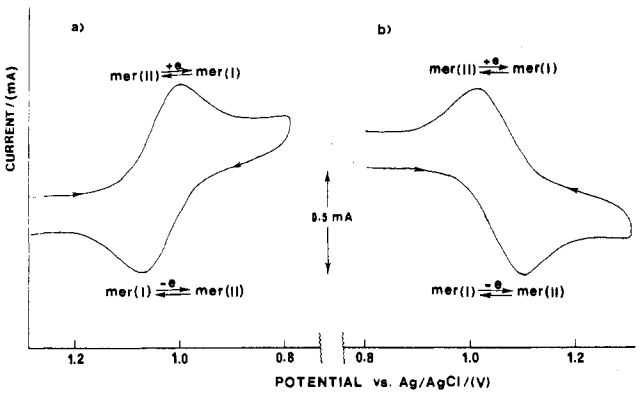

Figure 2. (a) Cyclic voltammogram of *mer*-$[Mn(CO)_3dpeBr]^+$ at 25 °C in acetonitrile (0.1 M Et_4NClO_4). Scan rate = 500 mV/s. (b) Cyclic voltammogram of *mer*-$Mn(CO)_3dpeBr$ at 25 °C in acetonitrile (0.1 M Et_4NClO_4). Scan rate = 500 mV/s.

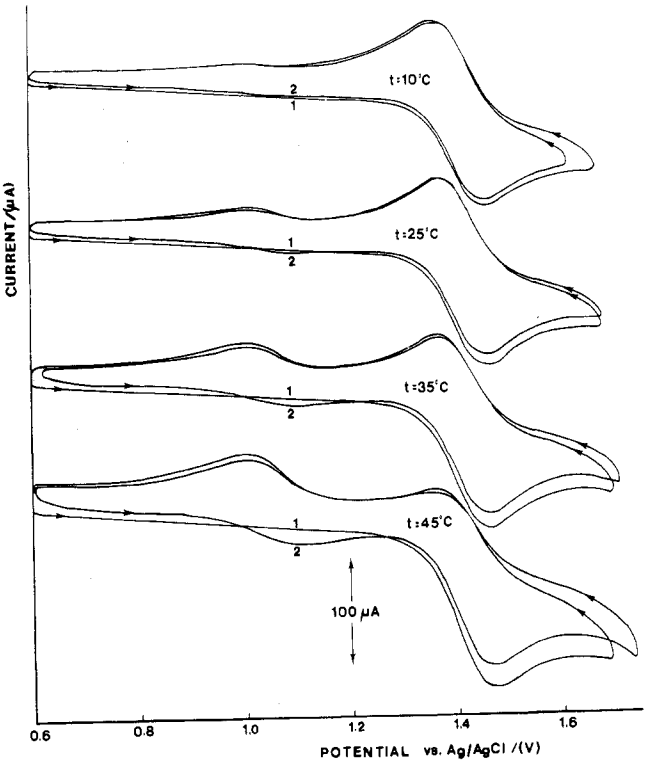

Figure 3. Temperature dependence of the cyclic voltammograms of *fac*-$Mn(CO)_3dpeBr$ in acetonitrile (0.1 M Et_4NClO_4). Scan rate = 500 mV/s.

step chronoamperometric method are presented in Table III. Data obtained for the $Mn(CO)_3dpmCl$ complex in a range of solvents at 25 °C are shown in Table IV and it can be seen that the rate of isomerism is not altered substantially in going from polar to nonpolar solvents. To ensure that cross redox reactions of the kind

fac-Mn(I) + *mer*-Mn(II) → *mer*-Mn(I) + *fac*-Mn(II)

and other reactions were not important, results obtained for k_1 via oxidation of *fac*-Mn(I) were repeated in the presence of *mer*-Mn(I) and *mer*-Mn(II). Rate constant data for solvolysis and solvent reduction of *mer*-Mn(II) (see later) show that these reactions are too slow to influence the measurement of k_1.

Electrochemical monitoring of the oxidation of a 10^{-2} M solution of *fac*-Mn(I) showed that $<10^{-4}$ M of *fac*-Mn(II) is present at the end of the electrolysis. This result proves that the equilibrium constant K_1 for the reaction

$$fac\text{-Mn(II)} \overset{K_1}{\rightleftharpoons} mer\text{-Mn(II)}$$

has a value of $\geq 10^2$ and that the back-reaction or isomerism

$$mer\text{-Mn(II)} \xrightarrow{k_1'} fac\text{-Mn(II)}$$

is negligible as assumed in the equation for the double potential step chronoamperometry.

Two likely mechanisms exist for the isomerism, *fac*-Mn(II) → *mer*-Mn(II). A twist mechanism would seem consistent with the k_1 solvent independence and the relative independence of k_1 on ligand substituents. Unfortunately, no nonelectrochemical data can be obtained to see if the complex is fluxional, but the slow electron-transfer step, k_{s_1}, may be consistent with rapid structural rearrangement (see above discussion). A dissociative bond-rupture mechanism, while also giving first-order kinetics, might be expected to be characterized by more marked substituent effects and/or solvent dependence of k_1 than has been observed. Obviously the dissociative mechanism cannot be excluded but the twist one is tentatively favored by the authors. Table V shows the activation parameters calculated from an Arrhenius plot of k_1 data contained in Table III. The enthalpy of activation is greater for chloride than for bromide and increases as arsenic replaces phosphorus in the bidentate ligand. Unfortunately, errors are too high to have much confidence in the entropies of activation, but it would appear that values become more negative when bromide replaces chloride and more positive as the arsenic content of the bidentate ligand increases. Speculation of the significance of these trends does not seem warranted in the absence of comparative examples of known mechanism.

(ii) *mer*-Mn(I) → *fac*-Mn(I). Examination of the $E_1°$, $E_2°$, and K_1 values suggests that the isomerism

$$mer\text{-Mn(I)} \xrightarrow{k_2} fac\text{-Mn(I)}$$

could be thermodynamically favored. However, spectrophotometric and electrochemical monitoring of the *mer*-$Mn(CO)_3dpeBr$ species for 24 h at 25 °C in acetonitrile showed that very slight decomposition (loss of CO) had occurred without isomerism. The corresponding dpm species decomposed faster[4] again without isomerism. Raising the temperature simply increases the rate of decomposition without enabling isomerism to be observed. In dichloromethane, the *mer*-Mn(I) species are completely stable over a 24-h period as are the *fac*-Mn(I) complexes with respect to isomerism in both acetonitrile and dichloromethane. These data imply a very high activation energy of isomerism occurs for 18e Mn(I) systems compared with the 17e Mn(II) systems. This may reflect the difference between a dissociative and twist mechanism in the different oxidation states. For the Mn-$(CO)_3(PR_3)_2X$ complexes studied by Angelici et al.[2] the direction of isomerism was cis → trans (with respect to PR_3

Table V. Enthalpies (ΔH^*) and Entropies (ΔS^* at 25 °C) of Activation for Isomerism of *fac*-$[Mn(CO)_3(L\text{-}L')X]^+$ in Acetonitrile (0.1 M Et_4NClO_4)

Compd (fac isomer)	ΔH^*, kJ mol^{-1}	ΔS^*, J K^{-1} mol^{-1}
$[Mn(CO)_3dpmCl]^+$	56 ± 4	−48 ± 14
$[Mn(CO)_3dpmBr]^+$	42 ± 4	−86 ± 13
$[Mn(CO)_3dpeCl]^+$	54 ± 19	−56 ± 60
$[Mn(CO)_3dpeBr]^+$	46 ± 10	−89 ± 32
$[Mn(CO)_3apeCl]^+$	76 ± 2	15 ± 5
$[Mn(CO)_3apeBr]^+$	54 ± 11	−57 ± 26
$[Mn(CO)_3daeCl]^+$	97[a]	93[a]
$[Mn(CO)_3daeBr]^+$	82 ± 8	37 ± 27

[a] Data obtained from only two points.

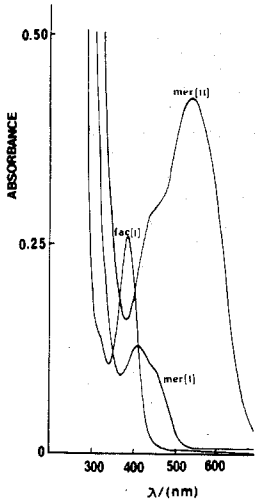

Figure 4. Visible spectra of *mer*-Mn(I), *mer*-Mn(II), and *fac*-Mn(I) in dichloromethane. Concentration of $[Mn(CO)_3dpeBr]^{0,+} = 2 \times 10^{-3}$ M. Cell path length = 1.0 mm.

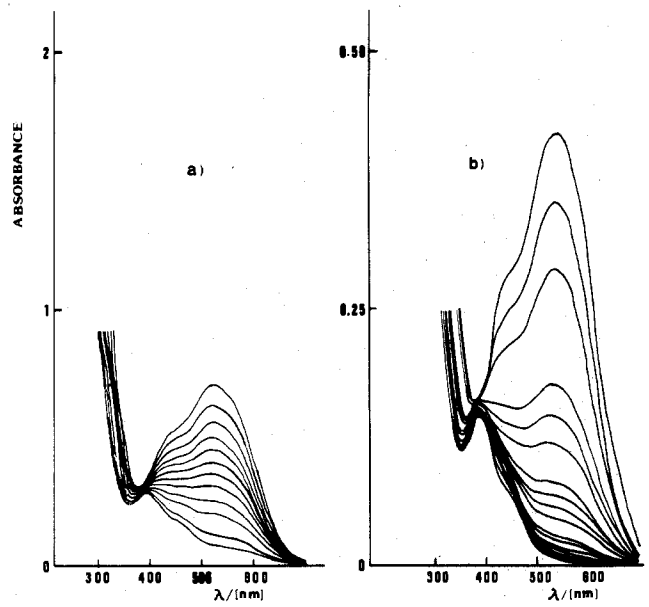

Figure 5. Decay of *mer*-$[Mn(CO)_3dpeBr]^+$ as a function of time in: (a) acetonitrile (0.1 M Et_4NClO_4), concentration = 4×10^{-4} M, cell path length = 10 mm; (b) dichloromethane (0.07 M Et_4NClO_4), concentration = 1.7×10^{-3} M, cell path length = 1.0 mm.

groups) and fac → mer (with respect to carbonyls) and rate constants are also extremely slow. Apparently the electronic configuration is important in reactions of carbonyl complexes with 18-electron systems being relatively kinetically inert compared with their 17-electron counterparts. Other evidence obtained from these laboratories[8,9] is consistent with this observation.

Other Reactions of *mer*-Mn(II) Complexes. Figure 4 shows the visible spectra of the three species that can be readily synthesized. The characteristic spectra and electrochemical behavior of each species readily enables the reactions of *mer*-Mn(II) with solvent to be monitored. Figure 5 shows the loss of *mer*-Mn(II) as a function of time in acetonitrile and dichloromethane in the dark. The kinetic data shown in Figure 6 are consistent with a first-order plot. Product analysis shows that in acetonitrile the *mer*-Mn(I) species is formed, while in dichloromethane a mixture of *mer*- and *fac*-Mn(I) isomers is produced. However, yields do not approach 100% and reactions other than simple oxidation of the solvent/supporting electrolyte and/or water impurity must be occurring. Repeating the experiment in Figure 5, again in the dark, but this

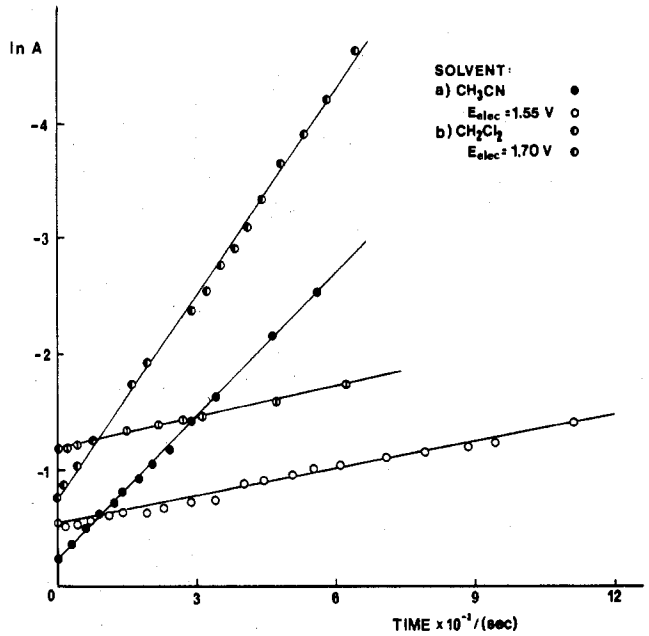

Figure 6. Kinetic data for the *mer*-$[Mn(CO)_3dpeBr]^+$ system in: (a) acetonitrile (0.1 M Et_4NClO_4), (b) dichloromethane (0.07 M Et_4NClO_4). A = absorbance.

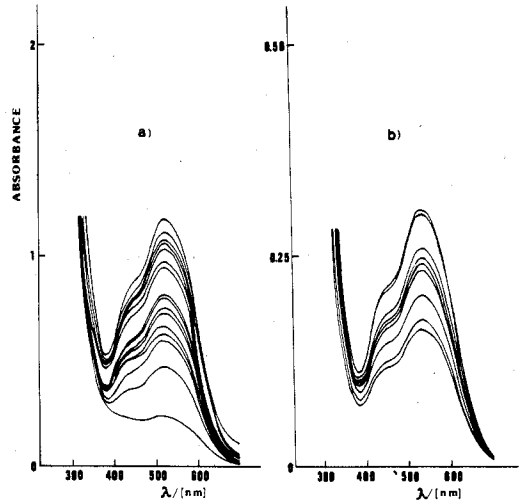

Figure 7. Decay of *mer*-$[Mn(CO)_3dpeBr]^+$ under an applied potential, E_{elec}, as a function of time in: (a) acetonitrile, $E_{elec} = +1.55$ V, concentration = 4×10^{-4} M, path length = 10 mm; (b) dichloromethane, $E_{elec} = +1.7$ V, concentration = 1.7×10^{-3} M, path length = 1.0 mm.

time in the presence of an electrode having an applied potential sufficient to oxidize any *mer*-Mn(I) or *fac*-Mn(I) species generated, and thereby quenching the redox step, gives the data obtained in Figure 7. On this occasion complete loss of CO is observed, and a first-order solvolysis reaction is demonstrated to be occurring in addition to the redox one (Figure 6). The observed first-order rate constant, k_{obsd}, obtained in the absence of the electrodes (Figure 6) therefore represents the sum of two processes (redox and solvolysis). In the presence of an

$$mer\text{-}[Mn(CO)_3(L\text{-}L')X]^+ \xrightarrow{\text{redox}} Mn(CO)_3(L\text{-}L')X \quad \text{(a)}$$

$$mer\text{-}[Mn(CO)_3(L\text{-}L')X]^+ \xrightarrow{\text{solvolysis}} Mn(II) + CO\uparrow \quad \text{(b)}$$

$$k_{obsd} = k_{red} + k_{solv}$$

electrode at an appropriate potential, any Mn(I) species generated by step a is immediately converted back to starting material, *mer*-$[Mn(CO)_3(L\text{-}L')X]^+$, at a much faster rate than

Table VI. Rates of Reaction of *mer*-$[Mn(CO)_3dpeBr]^+$ at 25 °C

Solvent	k_{obsd}, s^{-1}	k_{solv}, s^{-1}	k_{red}, s^{-1}
CH_3CN (0.1 M Et_4NClO_4)	$(4.12 \pm 0.03) \times 10^{-4}$	$(7.4 \pm 0.2) \times 10^{-5}$	3.38×10^{-4}
CH_2Cl_2 (0.1 M Et_4NClO_4)	$(5.8 \pm 0.2) \times 10^{-4}$	$(8.9 \pm 0.3) \times 10^{-5}$	4.91×10^{-4}

the other steps, so that k_{solv} can be measured in this experiment, k_{red} therefore can be calculated by subtraction of k_{solv} from k_{obsd}. Results obtained by linear least-squares analysis are summarized in Table VI.

During the course of the above measurements it was observed that *mer*-Mn(II) complexes are extremely light (visible) sensitive and on exposure to sunlight the purple *mer*-$[Mn(CO)_3(L\text{-}L')Br]^+$ or red *mer*-$[Mn(CO)_3(L\text{-}L')Cl]^+$ species are very rapidly reduced on the second time scale to yellow *mer*-$Mn(CO)_3(L\text{-}L')X$. In acetonitrile, yields of less than 100% are obtained but in dichloromethane close to 100% yield is found. Clearly, manganese(II) carbonyl species are extremely reactive and can undergo a large number of very interesting reactions which are considerably more complex than simple solvent reduction as has been proposed previously.[3,4] Many carbonyl complexes have been shown to be light sensitive.[10] Speculation of the light-sensitive pathway for catalyzing the redox reaction would in normal circumstances probably be that.[10]

$$mer\text{-Mn(II)} \xrightarrow{h\nu} fac\text{-Mn(II)}$$

Since the facial form is a much more powerful oxidant than the meridional one this would be consistent with the observations. However, reduction of *fac*-Mn(II) by solvent or water impurity should lead to the *fac*-Mn(I) complex, not the *mer*-Mn(I) form as found experimentally. An explanation of the transition state in the light-sensitive reaction must therefore await further detailed experimental examination.

Regardless of the mechanism of these reactions it seems clear that in addition to being kinetically labile with respect to isomerism (as noted previously) the 17-electron systems are labile with respect to a wide range of reactions. Studies of other manganese and rhenium 17-electron systems[11,12] also indicate that facile substitution of CO is a characteristic of their chemistry so this observation may be of fairly general applicability.

Acknowledgment. The financial assistance of the Australian Research Grants Committee, support from Melbourne University in the form of a Postdoctoral Research Fellowship for B.S.G., and many valuable discussions with Dr. Ray Colton are all gratefully acknowledged by the authors.

Registry No. $[Mn(CO)_3dpmCl]^+$ (*mer*), 60305-99-9; $[Mn(CO)_3dpmBr]^+$ (*mer*), 60325-42-0; $[Mn(CO)_3dpeCl]^+$ (*mer*), 65634-87-9; $[Mn(CO)_3dpeBr]^+$ (*mer*), 65634-86-8; $[Mn(CO)_3apeCl]^+$ (*mer*), 65622-62-0; $[Mn(CO)_3apeBr]^+$ (*mer*), 65622-61-9; $[Mn(CO)_3daeCl]^+$ (*mer*), 65622-60-8; $[Mn(CO)_3daeBr]^+$ (*mer*), 65622-59-5; $[Mn(CO)_3dpmCl]^+$ (*fac*), 65634-85-7; $[Mn(CO)_3dpmBr]^+$ (*fac*), 47752-42-1; $[Mn(CO)_3dpeCl]^+$ (*fac*), 65622-58-4; $[Mn(CO)_3dpeBr]^+$ (*fac*), 47768-35-4; $[Mn(CO)_3apeCl]^+$ (*fac*), 65634-91-5; $[Mn(CO)_3apeBr]^+$ (*fac*), 65634-90-4; $[Mn(CO)_3daeCl]^+$ (*fac*), 65634-89-1; $[Mn(CO)_3daeBr]^+$ (*fac*), 65634-88-0.

References and Notes

(1) On leave from the Faculty of Technology, University of Zagreb, Zagreb, Yugoslavia.
(2) R. J. Angelici, F. Basolo, and A. J. Pol, *J. Am. Chem. Soc.*, **85**, 2215 (1963).
(3) R. H. Reimann and E. Singleton, *J. Organomet. Chem.*, **38**, 113 (1972).
(4) A. M. Bond, R. Colton, and M. J. McCormick, *Inorg. Chem.*, **16**, 155 (1977).
(5) W. M. Schwarz and I. Shain, *J. Phys. Chem.*, **69**, 30 (1965).
(6) R. Colton and M. J. McCormick, *Aust. J. Chem.*, **29**, 1657 (1976).
(7) S. W. Feldberg and A. J. Bard, Ed., "Electroanalytical Chemistry", Vol. 3, Marcel Dekker, New York, N.Y., 1959, pp 195–296.
(8) F. L. Wimmer, M. R. Snow, and A. M. Bond, *Inorg. Chem.*, **13**, 1617 (1974).
(9) A. M. Bond, R. Colton, and J. J. Jackowski, *Inorg. Chem.*, **14**, 274 (1975).
(10) M. Wrighton, *Chem. Rev.*, **74**, 401 (1974).
(11) B. H. Byers and T. L. Brown, *J. Am. Chem. Soc.*, **99**, 2527 (1977), and references cited therein.
(12) D. S. Ginley, C. R. Bock, and M. S. Wrighton, *Inorg. Chim. Acta*, **23**, 85 (1977).

Contribution from the School of Chemical Sciences, University of East Anglia, Norwich, NR4 7TJ, United Kingdom

Solid-State Studies. 10. Vibrational Spectra of Mixed and Isotopic Crystals of Manganese and Rhenium Pentacarbonyl Iodides

DAVID N. KARIUKI and SIDNEY F. A. KETTLE*[1]

Received August 17, 1977

The Raman spectra of mixed crystals of manganese and rhenium pentacarbonyl iodides and of ^{13}CO-enriched manganese pentacarbonyl iodide are interpreted in terms of one-mode, intermediate, and two-mode behaviors, notwithstanding the absence of overt factor group splitting in the individual spectra of the pure compounds.

The majority of work which has been reported on the composition dependence of the vibrational spectra of crystals containing components of which the relative proportions may be varied over a wide range has been concerned with semiconductor, alloy, and ionic crystals.[2] Such studies have therefore been concerned with the behavior of the long-wavelength optical phonons. Two types of behavior have been recognized. In the first, cases exhibiting so-called one-mode behavior, the frequency of the spectral feature varies continuously and approximately linearly with concentration from the frequency characteristic of one pure component to that of the other. The band intensity remains approximately constant. Examples of mixed crystals belonging to this class include compounds which might normally be regarded as ionic.[2b-10]

In the other class of mixed-crystal vibrational behavior, the so-called two-mode type, two phonon features are observed, each frequency being close to that associated with one of the pure components. The intensity of each varies continuously from its maximum (for one end member) to zero as its fractional contribution varies from 1 to 0 or from 0 to 1. Examples of mixed crystals belonging to this category tend to be those that might be regarded as covalent materials.[11-15] In some cases both one- and two-mode behaviors have been found.[16] For both types it has been observed that spectral line widths increase with concentration exhibiting a maxium near

0020-1669/78/1317-1018$01.00/0